European Space Agency

DETECTION OF CLOUDS FOR PROBA–V

Algorithm Theoretical Basis Document (ATBD)

Issue 1.0, 21.03.2017

prepared by
Rene Preusker and Jürgen Fischer

Document, Version	Date	Changes	Originator
ATBD, v1.0	21.03.2017	Original	Jürgen Fischer, Rene Preusker

Table of Content

ACRONYMS AND ABBREVIATIONS **3**

REFERENCES **4**

1 INTRODUCTION **5**

1.1 PURPOSE 5

2 BACKGROUND AND ALGORITHM OVERVIEW **5**

2.1 PROBA-V 5

2.2 NAMING CONVENTIONS 5

2.3 ALGORITHM OVERVIEW 6

3 ALGORITHM DESCRIPTION **7**

3.1 THEORETICAL DESCRIPTION 7

3.1.1 Physic of the problem *7*

3.1.2 Cloud optical thickness *8*

3.2 PRACTICAL CONSIDERATIONS 9

3.2.1 Radiative transfer simulations *9*

3.2.2 Estimation of cloud optical thickness *9*

3.2.3 Cloud free restoral test *10*

3.2.4 Cloud detection sequence and thresholds *10*

3.3 INPUT AND OUTPUT DATA 10

3.4 PROGRAMMING 11

4 ASSUMPTIONS AND LIMITATIONS **11**

5 CONCLUSIONS **11**

Acronyms and Abbreviations

ANN	Artificial neural network
ATBD	Algorithm Theoretical Basis Document
COT	Cloud optical thickness
Envisat	ESA satellite (see http://envisat.esa.int/)
ESA	European Space Agency (http://www.esa.it/export/esaCP/index.html)
ESTEC	European Space Research and Technology Centre
ESRIN	European Space Research Institute (http://www.esa.it/export/esaCP/index)
FUB	Free University Berlin
FoV	Field of View
L1/L2	Level 1 / Level 2
LBL	Line-by-line
LUT	Look-up table
MERIS	Medium Resolution Imaging Spectrometer Instrument (http://envisat.esa.int/)
MLP	Multi Layer Perceptron
MODIS	Moderate Resolution Imaging Spectroradiometer (on board the NASA EOS-Aqua satellite)
MOMO	Matrix Operator Modell
NASA	National Aeronautics and Space Administration
RTC / RTM	Radiative Transfer Code / Model
TOA	Top of atmosphere

References

Applicable Documents

[AD-1]	Erwin Wolters, Wouter Dierckx, Marian-Daniel Iordache, and Else Swinnen: PROBA-V Products User Manual, Version: 2.1, Date: 6/02/2017 http://proba-v.vgt.vito.be/sites/default/files/PROBAV-Products_User_Manual_v2.1.pdf

Reference Documents

[RD-1]	F. Fell and J. Fischer. Numerical simulation of the light field in the atmosphere ocean system using the matrix-operator method. Journal of Quantitative Spectroscopy and Radiative Transfer, 69(3):351 – 388, 2001. Hollstein, André and Jürgen Fischer, 2012: Radiative transfer solutions for coupled atmosphere ocean systems using the matrix operator technique. Journal of Quantitative Spectroscopy and Radiative Transfer Volume 113, Issue 7, May 2012, Pages 536–548, 2012.
[RD-2]	Cox, C. and Munk, W.: Measurement of the Roughness of the Sea Surface from Photographs of the Sun‘s Glitter, J. Opt. Soc. Am.,44, 838–850, 1954
[RD-3]	Auer, Peter; Harald Bergsteiner; Wolfgang Maass (2008). "A learning rule for very simple universal approximators consisting of a single layer of perceptrons"
[RD-4]	American Meteorological Society, Glossary of Meteorology. [Available online at http://glossary.ametsoc.org/wiki/]
[RD-5]	Muller, J.-P., Preusker, R., Fischer, J., Zuhlke, M., Brockmann, C., and Regner, P.: ALBEDOMAP: MERIS land surface albedo retrieval using data fusion with MODIS BRDF and its validation using contemporaneous EO and in situ data products, in: Geoscience and Remote Sensing Symposium, 2007, IGARSS, 2007,IEEE International, 2404–2407, 2007
[RD-6]	Fischer J., R. Preusker, and L. Schueller. ATBD cloud top pressure. Algorithm Theoretical Basis Document PO-TN- MEL-GS-0006, European Space Agency, 1997.
[RD-7]	King, M. D., S. C. Tsay, S. E. Platnick, M. Wang and K. N. Liou, 1997: Cloud Retrieval: Algorithms for MODIS: Optical Thickness, Effective Particle Radius, and Thermodynamic Phase. Algorithm Theoretical Basis Document ATBD-MOD-05, 79 pp.
[RD-8]	Dee, D. P., Uppala, S. M., Simmons, A. J., Berrisford, P., Poli, P., Kobayashi, S., Andrae, U., Balmaseda, M. A., Balsamo, G., Bauer, P., Bechtold, P., Beljaars, A. C. M., van de Berg, L., Bidlot, J., Bormann, N., Delsol, C., Dragani, R., Fuentes, M., Geer, A. J., Haimberger, L., Healy, S. B., Hersbach, H., Hólm, E. V., Isaksen, L., Kållberg, P., Köhler, M., Matricardi, M., McNally, A. P., Monge-Sanz, B. M., Morcrette, J.-J., Park, B.-K., Peubey, C., de Rosnay, P., Tavolato, C., Thépaut, J.-N. and Vitart, F. (2011), The ERA-Interim reanalysis: configuration and performance of the data assimilation system. Q.J.R. Meteorol. Soc., 137: 553–597. doi: 10.1002/qj.828
[RD-9]	Schröder, M., R. Bennartz, L. Schüller, R. Preusker, P. Albert and J. Fischer, 2002: Generating cloudmasks in spatial high-resolution observations of clouds using texture and radiance information. Int. J. Remote Sensing, 23, 4247-4261.
[RD-10]	Carroll, M.L.; Townshend, J.R.; DiMiceli, C.M.; Noojipady, P.; Sohlberg, R.A. A new global raster water mask at 250 m resolution. Int. J. Digit. Earth 2009, 2, 291–308.
[RD-11]	C. B. Schaaf, F. Gao, A. H. Strahler, W. Lucht, X. Li, T. Tsang, N. C. Strugnell, X. Zhang, Y. Jin, J.-P. Muller, P. Lewis, M. Barnsley, P. Hobson, M. Disney, G. Roberts, M. Dunderdale, C. Doll, R. d'Entremont, B. Hu, S. Liang, J. L. Privette, "First Operational BRDF Albedo and Nadir Reflectance Products from MODIS", Remote Sens. Environ., vol. 83, pp. 135-148

1 Introduction

1.1 Purpose

This document provides information about the physical background, technical structure and the functional principle of a cloud detection algorithm for PROBA-V level2a data.

2 Background and algorithm overview

2.1 Proba-V

PROBA-V was developed as both a follow-up to the 15-year SPOT-VEGETATION mission, as well as a preparation for the upcoming ESA Sentinel-3 land and ocean observation satellite mission. PROBA-V's spectral channels are similar to those of the SPOT-VGT instrument to preserve observational consistency with the SPOT-VGT. Using a constellation of 3 cameras, PROBA-V covers the entire Earth every two days and provides useful reflectance measurements for climate impact assessment, surface water resource management, agricultural monitoring, and food security purposes.

The Proba-V *vegetation* instrument consists of three almost identical units, each having a field of view of about 34.8°, has three channels with a spatial resolution of 330 m in the VIS/NIR and one in the SWIR with 660 m spatial resolution (Table 1, AD-1).

Table 1: Technical specification of Proba-V.

Proba-V Vegetation instrument	**Specification**
3 compact, wide field of view, 3-mirror Astigmatic telescope	(3x 34.6°) x 5.5°
Visual and Near InfraRed detectors	3x 5200 pixels, 13 µm
Blue band (BLUE)	447–493 nm
Red band (RED	610–690 nm
Near infrared band (NIR)	777–893 nm
Ground resolution	~ 333 m
Short Wave InfraRed detector	3x 1024 pixels, InGaAs detectors
Short wave infrared band (SWIR)	1570–1650 nm
Ground resolution	~ 666 m

The quality of the Proba-V products is a key element to guarantee the achievement of the objectives of the mission, which are related to the monitoring of the land use and land cover and also to the understanding of the long term behaviour of the vegetation. The production of multi temporally composited cloud-free mosaics of land surfaces is crucial to yield information for the study of terrestrial vegetation structure and dynamics, and land cover mapping.

2.2 Naming conventions

There is a slight vagueness of nomenclature in the context of cloud detection. Within this document we use the following terms:

- **Cloud detection**: the full process that results in a per-pixel cloud or cloud free (probability or portion) quantification. This could be binary (cloudy/cloud free), multi class categorical (yes/unknown/no or yes/propbaly/probably_not/no) or continuous measure (probability of cloud contamination or probability of cloud free or cloud coverage)

- **Cloud mask**: a binary mask (in the same projection of the satellite image) where pixel with a distinct cloud incidence (e.g. probably cloudy or cloud contaminated or cloud free or probably cloud free or ...) are masked out. Cloud masks are sometimes classified as
    - cloud free conservative for applications that do not allow cloud contamination (e.g. the remote sensing of land-, sea- and ice surface temperatures, of total column water vapour or of aerosol optical properties),
    - cloud conservative for most cloud remote sensing applications and
    - climatologically conservative which means that they should not be biased in particular with respect to instrumental improvements or calibration changes within decades.
- **(Cloud) flags**: a bit-field (in the same projection of the satellite image) where any kind of additional information (e.g. thin cloud, cloud border, inconsistent data, …) is stored.
- **Cloud test**: A cloud test is a test for a distinct physical cloud or cloud free feature, e.g. brightness or temperature or spectral index that results in a single measure.

2.3 Algorithm overview

The Proba-V instrument, having only four relatively broad bands in the VIS, NIR and SWIR spectral region, is not well suited to detect clouds, since no thermal contrast is observable. Only few spectral and spatial features of clouds can be used. For the herein described cloud detection algorithm, we decided to use spectral features alone, and to a certain extend temporal features, but no spatial features, since we want to abstain from training data which is often manually generated and subjective.

Essentially the cloud detection is based on a single test only: *a pixel is cloudy, if the cloud optical thickness COT is larger than a specific threshold*. The approach has several advantages and disadvantages as follows. The advantages are:

- The cloud test is closely related to the definition of a cloud:
    - The cloud optical thickness is proportional to the amount of cloud water (see section 3.1.2)
    - The cloud optical thickness threshold is related to the preceptional skill of the instrument: If the cloud optical thickness is below the detection limit, the cloud is invisible, and by the upper definition not a cloud.
- The cloud test is *objective* in a way that a physical parameter is tested, which could be validated independently. Cloud optical thickness is a well defined quantity and can be retrieved from many different satellite or from ground based measurements.
- The cloud test is comparable with different sensors, if the same COT threshold is used.
- The significance of a certain COT threshold can easily be assessed by downstream algorithms. E.g. whether the calculation of NDVI or an atmospheric correction is or is not disturbed significantly by a thin cloud, can be quantified by radiative transfer simulations.
- The test is conceptually simple, easy to maintain and easy to transfer to different instruments. Cloud detections based on decision trees tend to evolve and to become difficult to maintain because of side effects of threshold changes.

Disadvantages:

- The information from spatial features is not used. Cloud textures could be used in valuable cloud tests but needs appropriate feature recognition and careful evaluation.
- The cloud test can hardly discriminate thick aerosols from thin clouds.
- The estimation of the cloud optical thickness depends strongly on the assumed surface

brightness, in particular for thin clouds. Several sources are possible, we tested:
  - MERIS albedo map climatology [RD-5]
  - Actual MODIS 16 day albedo [RD-11] or derived albedo climatology

The uncertainty and errors of these databases went directly into the uncertainty of the cloud optical thickness estimation.

For land surfaces the COT is calculated from the RED band (since the influence of vegetation is less) and for water surfaces the COT calculated from the NIR band (since the influence of aerosol and Rayleigh scattering is less and above all the water leaving radiance is negligible). The COT estimation is currently a regression based inversion of pre-calculated look up tables derived from radiative transfer calculations using the radiative transfer code MOMO [RD-1].

3 Algorithm description

3.1 Theoretical description

3.1.1 Physic of the problem

“A visible aggregate of minute water droplets and/or ice particles in the atmosphere above the earth’s surface” [RD4] is what is commonly called a cloud. The crucial adjective in the context of cloud masking for satellite remote sensing is **visible**, because whether a cloud is visible and important for an instrument depends on the instruments characteristics, spectral channels and radiometry, as well as on downstream algorithms and **not** on the cloud itself! (Most LIDAR instruments detect water particles down to an optical thickness of 0.05 whereas flight SAR systems see only heavy rain or snow)

Eventually all different cloud detection methods developed for satellite imagery rely on a *contrast* between a cloud free, a cloud contaminated and/or a cloudy *feature set*. This feature set can contain:

1. *Spectral features*. The radiative transfer in the Earth atmosphere is driven by absorption and emission of gases, scattering, absorption and emission by air-molecules, aerosol and cloud particles. Depending on wavelength, all constituents interact with the radiation differently, but sometimes likewise. Additionally, the radiation properties of the land and ocean surface have a significant impact on the radiation as measured by a satellite instrument. Thus, a cloud is only one of many factors. Radiative features of a cloud are:
   a. brightness and whiteness in the VIS/NIR,
   b. shielded atmospheric absorption in the VIS/NIR
   c. shielded spectral surface features (e.g. NDVI)
   d. shielded atmospheric emission in TIR
   e. spectral features of scattering, absorption and emission (dust vs. water clouds vs. ice clouds)
   f. spectral features of emission (split window methods)
2. *Spatial features,* using the fact that the apparent texture of clouds differs from the texture of the underlying surface, e.g.:
   a. standard deviation of apparent brightness temperatures or reflectance above sea surfaces within a macro pixel.
   b. linear features for detecting contrails.
   c. more sophisticate texture measures like all quantities, that can be calculated from the grey level co-occurrence matrices *(entropy , homogeneity)*

   However, these tests are sensor / resolution / observation specific and need a high amount of training data.
3. *Temporal features*, using the fact that clouds can change the top of atmosphere radiance very fast. These tests are only applicable, if the same object is observed several times:
   a. from geostationary orbits
   b. from time series

   c. from polar orbiter at high latitudes
4. *Indirect tests*, that do not directly use cloud features
   a. polar night cloud detection. Some tests are using the suppressed radiative cooling of the surface, if clouds are present
   b. non-converging downstream retrievals. Here the presence of a cloud is assumed, if a L2 algorithm (e.g. sea surface temperature) is not converging or produces unlikely results.

3.1.2 Cloud optical thickness

The fundamental quantity of the cloud detection algorithm described herein is the cloud optical thickness. The cloud optical thickness is defined as:

$$COT = \int_{base}^{top} \sigma_{ext}(h)\, n(h)\ dh\ ,$$

the integral over the cloud droplet extinction cross section σ [m^2] multiplied by the cloud droplet number concentration n [$1/m^3$]. For homogenous clouds with cloud droplets having particle radius *r,* and assuming that the extinction cross section in the VIS and NIR spectral range can be approximated by

$$\sigma_{ext} = 2 \cdot \pi\, r^2\ ,$$

the equation simplifies to:

$$COT = \frac{3}{2} \cdot \frac{L}{\rho \cdot r}\ ,$$

with the cloud liquid water column L in [kg/m^2] and the water density ρ [kg/m^3]. There is virtually no spectral dependence of the extinction cross section between RED and NIR for clouds, consequently the cloud optical thickness is the same in both bands. For more realistic clouds, this simple equation is not valid anymore, but the main dependency remains: the cloud optical thickness is directly proportional to the amount of liquid (or ice) water in the cloud and independent on the wavelength (concerning RED and NIR).

The relation between cloud optical thickness and the measured top of atmosphere reflectance *ref* is more complicated and can only be tackled by radiative transfer simulations. However, in principal it meets the following equation:

$$ref = a + \frac{b \cdot COT}{c + COT}\ ,$$

where the coefficients *a, b* and *c* depend on surface, viewing and sun geometry, cloud microphysics, cloud height, potentially trace gas amounts etc.

To summarize: the top of atmosphere brightness of a pixel is *monotonically* dependent on the amount of cloud water. The precise relation between brightness and cloud water can be calculated using full radiative transfer theory. This is not surprising; however, if the relation between cloud water and brightness is monotonic and further for low COT's almost linear, then the estimation of the COT from the measured top of atmosphere brightness is a simple inverse problem. This is illustrated in Figure 1, showing the relation between TOA reflectance, cloud optical thickness and surface albedo.

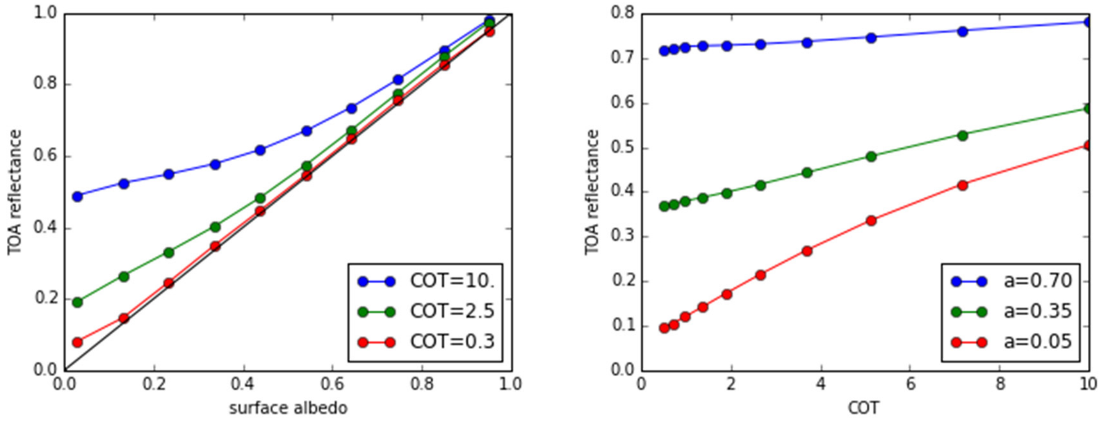

Figure 1: Simulated TOA reflectance for several combinations of cloud optical thickness (COT) and surface albedo (a).

3.2 Practical considerations

3.2.1 Radiative transfer simulations

Radiative transfer simulations have been performed to create the data for the inversion process. They cover the whole range of possible conditions and account for all parameters and processes, affecting the retrieval. The most important are:

- COT between 0 and 50
- Cloud top height between 1000 hPa and 200 hPa
- White sky surface albedo between 0 and 1 for land simulations
- Wind speed between 3 m/s and 15 m/s for sea simulations
- Sun and viewing zenith between 0 and 76°, relative azimuth between 0° and 180°

In total 15 million simulated measurements have been created and used for the training and test of the cloud optical thickness regression.

3.2.2 Estimation of cloud optical thickness

The COT is estimated from the top of atmosphere reflectance by a multidimensional non-linear regression, implemented as multi-layer-perceptron artificial neural network (MLP). A multilayer perceptron can be written as a sequence of linear transformations (dot product with weight matrices W_i) and nonlinear transformations σ (e.g. sigmoidal function or a tangent hyperbolic) of an input vector I. For numerical reasons the input is scaled by S_i to ranges e.g between 0 and 1 or to a normalized variance, and the output is scaled by S_o back from a range between 0 and 1 (or -1 and 1 if tangent hyperbolic is used as nonlinear transformation) to physical quantities.

$$COT = S_o\left(\sigma\left(W_n \cdot \sigma\left(W_{n-1} \cdot \sigma(\ldots\ W_1 \cdot S_i(I))\right)\right)\right)$$

The scaling parameter and optimal weights are found by the *training* of the network [described e.g. here: RD-3] using a subset of the simulated data. The input vector I consists of 4 elements: [top of atmosphere reflectance, sun zenith, viewing zenith, azimuth difference, surface albedo], the output vector has one element only: the cloud optical thickness COT.

Remark 1: The cloud optical thickness is calculated and used as log10 scaled.

Remark 2: It is not necessary and crucial to use a MPL for the estimation of the COT. Any other inverse method could be used. E.g. for the COT estimation in MERIS a simple polynomial has been used, the coefficients however had to be interpolated to observation geometry and surface properties [RD6]. MODIS standard retrievals use maximum likelihood estimators [RD-7]. MLPs have the advantage to be fast and very easy to implement.

3.2.3 Cloud free restoral test

Ice clouds and snow share many common properties and are very hard to discriminate. The *normalized difference snow index NDSI:*

$$NDSI = \frac{RED - SWIR}{RED + SWIR}$$

can be used to detect snow, since it indicates the presence of ice. But, unfortunately it works for both: ice clouds and snow. In particular, deep convective clouds show the same spectral features as snow (using PROBA-V bands). The amount of false snow alarms can largely be removed, if the test is only applied for situations, where snow can be present. We identify these situations by a simple threshold of the surface temperature obtained from meteorological analysis [RD-8]

3.2.4 Cloud detection sequence and thresholds

The cloud detection sequence works as follows (on a pixel-by-pixel basis):

1. Interpolation/sampling of all auxiliary data to PROBA-V pixel location and acquisition time:
    a. Land sea mask [RD-10]
    b. RED surface albedo [RD-11]
    c. NIR surface albedo [RD-11]
    d. Wind speed [RD-8]
    e. Surface temperature [RD-8]
2. Calculation of RED and NIR COT (section 3.2.2)
3. Flagging **cloud** if RED or NIR COT (if land or sea resp.) is above *TH_cloud*
4. Calculation of NDSI if **cloud** and surface temperature is below temperature threshold *TH_temp_land* or *TH_temp_sea* resp.
5. Cloud free restoral (unflagging **cloud** and flagging **snow**) if NDSI is above threshold *TH_ndsi*
6. Flagging **COT-inconsistency** if **cloud**, but COT NIR and COT RED differ more than threshold *TH_inconsistency*. The COT inconsistency is quantified by:

$$abs(1. - COT\_RED/COT\_NIR)$$

7. Flagging **thin cloud** if **cloud** but COT is below threshold *TH_thin*

The currently used thresholds are (cloud optical depths are in *log10* space):

1. Cloud detection threshold *TH_cloud* = 0.0 (belongs to an optical thickness of 1)
2. Temperature threshold *TH_temp_land*= 10°C, *TH_temp_sea*= 0°C
3. Snow restoral *TH_ndsi* = 0.45
4. Inconsistency warning *TH_inconsistency* = 0.2
5. Thin cloud flagging *TH_thin* = 0.3 (belongs to an optical thickness of 2)

3.3 Input and Output data

The used PROBA-V data are level 2a. The files contain top of atmosphere quantities (mainly reflectance, geometry and flags) [AD-1], projected on a common WGS84 latitude – longitude grid. The cloud detection processor is using the normalized reflectances as provided (definition see table 2). The observation geometry is expressed as viewing zenith angle, Sun zenith angle and azimuth difference angle.

Auxiliary data is used from ECMWF analysis (surface temperature, wind speed at ground) [RD-8], land surface albedo MOD43 [RD-11] and land sea mask MOD44 [RD-10]. All auxiliary data is preparatory converted into NetCDF4, to simplify the processor architecture. All meteorological data and the surface albedo are 3D linearly interpolated (lon, lat, time) to the actual pixel position and observation time, the land sea mask and elevation are nearest-neighbour sampled.

Table 2: Satellite measurements taken from the Level 2a instrument data files.

Quantity	Unit	Valid range	Source	Comment
Reflectance: RED, NIR, SWIR	1	0 -1	L2a	Reflectance is defined as: $\frac{L \cdot \pi}{cos(\theta_{sun}) \cdot F_{sun}}$, with L the measured top of atmosphere radiance, and *F* the band averaged solar irradiance (corrected for earth orbit eccentricity)
Viewing zenith angle: θ_{view}	deg	0-60	L2a	
Sun zenith angle: θ_{sun}	deg	0-75	L2a	
Azimuth difference angle: ϕ	deg	0-180	L2a	

Table 3: Auxiliary data and valid range used in the CTP processor.

Quantity	Unit	Valid range	Source	Comment
Surface albedo RED and NIR	1	0-1	NASA, RD-11	Modis 16 day should be used as it is considered as best source
Land sea mask	1	0, 1	NASA, RD-10	
Surface temperature	K	260 - 330	ECMWF, RD-8	
Wind speed	m/s	0 - 20	ECMWF, RD-8	

Table 4: Output data

Quantity	Unit	Valid range	Comment
COT	1	-0.4 – 2.5	In Log10 space, intermediate data for debugging purpose only and currently not saved
Cloud mask flags	1	0 - 255	

3.4 Programming

The processor is coded in almost pure python using the numpy extension only. For input and output, NetCdf4 and hdf5 extensions are used additionally (only the currently latest version *2.6* of h5py works with PROBA-V level2a data).

4 Assumptions and limitations

The estimation of the cloud optical thickness depends strongly on the knowledge of the surface albedo. This virtually shifts the cloud detection towards MODIS which has capabilities much better for cloud detection. The assumption of negligible water leaving radiance in the NIR is not valid for highly scattering, sediment loaded waters. Here the SWIR band should be used.

5 Conclusions

The Proba-V cloud detection is functional, efficient and produces good results. Nevertheless, further improvements should consider cloud textures and the SWIR band measurements.